MANEUVER REGULATION AND STABILITY ANALYSIS FOR AUTONOMOUS REDUCED-G FLIGHT USING TRIPLE INTEGRAL CONTROL

DECISION & CONTROL LABORATORY
dcl.gatech.edu

GEORGIA Space Grant Consortium

Georgia Tech Institute for Robotics and Intelligent Machines

University of Colorado Boulder

JOHN HAUSER

+ PABLO AFMAN & ERIC FERON

NASA

THE UNIQUENESS OF THIS PROGRAM AIMS AT THE **DEVELOPMENT OF AN AUTONOMOUS PLATFORM** THAT **COSTS LESS THAN A SINGLE PARABOLIC FLIGHT**, AND CAN **PROVIDE APPROPRIATE REDUCED-GRAVITY ENVIRONMENTS** TO STUDENTS, RESEARCH INSTITUTIONS, AND PRIVATE ORGANIZATIONS.

WHY DO WE CARE ABOUT PARABOLIC FLIGHTS?

PARABOLIC FLIGHTS ENABLE THE STUDY OF PHYSICAL SYSTEMS IN REDUCED GRAVITY CONDITIONS

MARTIAN RESEARCH

LUNAR RESEARCH

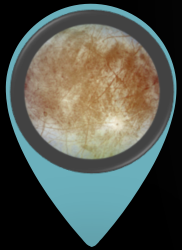

EUROPA RESEARCH

MICROGRAVITY RESEARCH

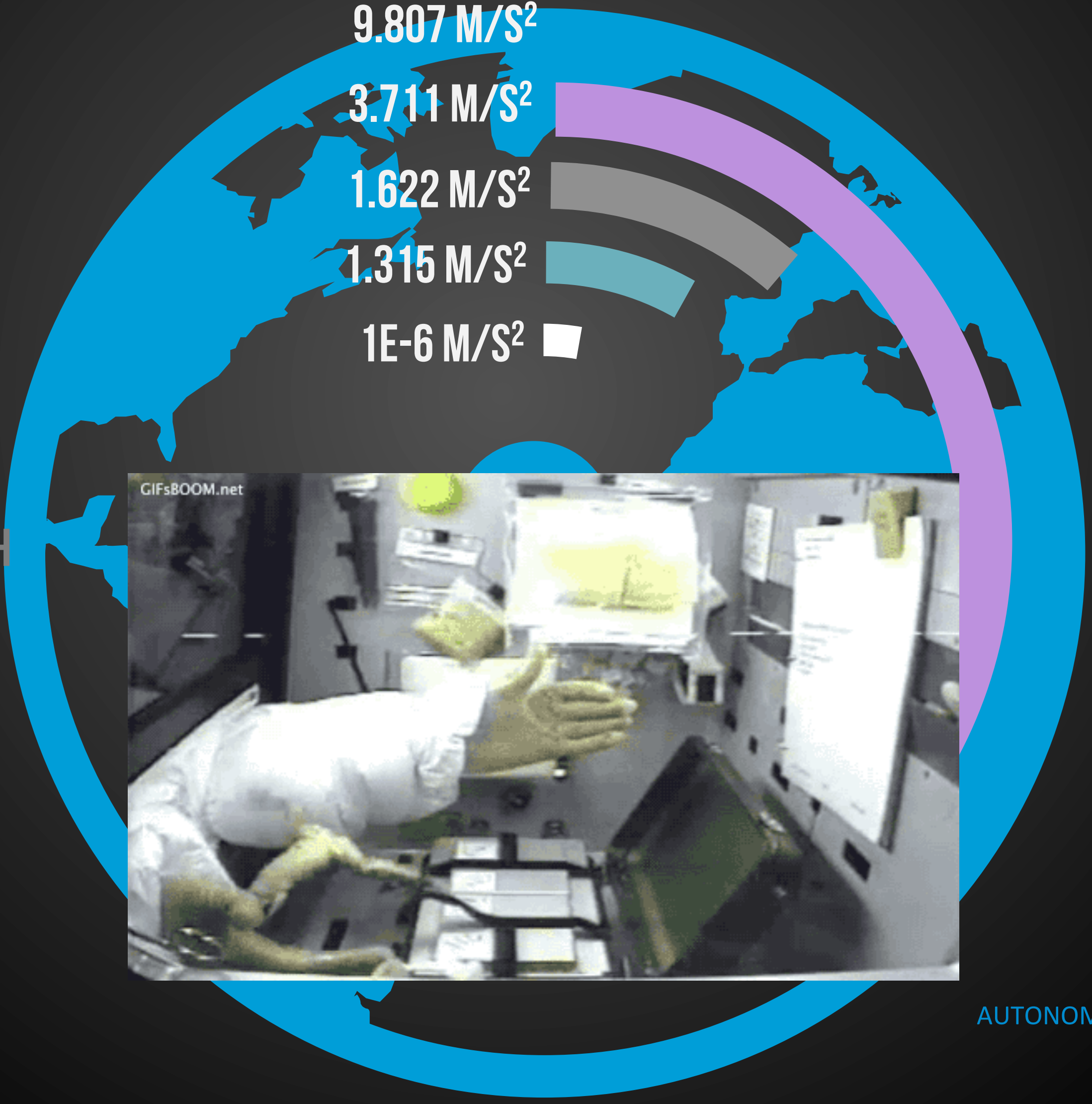

PHYSICAL PROCESSES, *AS WE KNOW THEM*, BEHAVE VERY DIFFERENTLY UNDER THE ABSENCE OF A GRAVITATIONAL FIELD.

FOR EXAMPLE, FLAMES PROPAGATE SPHERICALLY DUE TO NEGLIGIBLE BUOYANCY FORCES.


zero G
BLUE ORIGIN

REVIEW OF PRIOR ART

A 22 YEAR-OLD UNSOLVED CHALLENGE

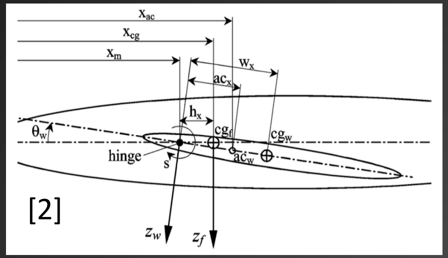

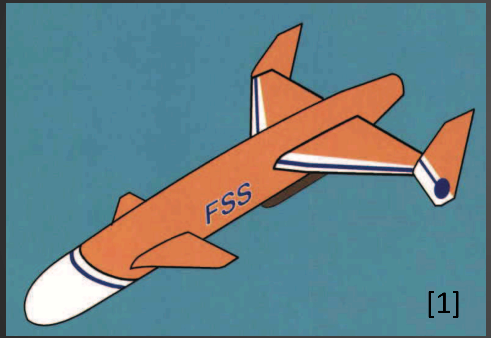

[1] MESLAND, D., ET AL. "BALLISTOCRAFT: A NOVEL FACILITY FOR MICROGRAVITY RESEARCH." ESA BULLETIN. BULLETIN ASE. EUROPEAN SPACE AGENCY 82 (1995): 7-P.
[2] KRAEGER, ALWIN M. "FREE-WING UNMANNED AERIAL VEHICLE AS A MICROGRAVITY FACILITY." JOURNAL OF GUIDANCE CONTROL AND DYNAMICS 29.3 (2006): 579.
[3] HOFMEISTER, PAUL GERKE, AND JÜRGEN BLUM. "PARABOLIC FLIGHTS@ HOME." MICROGRAVITY SCIENCE AND TECHNOLOGY 23.2 (2011): 191-197.
[4] HIGASHINO, SHINICHIRO, AND SHOTARO KOZAI. "AUTOMATIC MICROGRAVITY FLIGHT SYSTEM AND FLIGHT TESTING USING A SMALL UNMANNED AERIAL VEHICLE." J. JPN. SOC. MICROGRAVITY APPL. VOL 27.1 (2010): 3-10.
[5] JOHNSON SPACE CENTER, "UNMANNED MICROGRAVITY FLIGHT PROGRAM". BIENNIAL RESEARCH AND TECHNOLOGY DEVELOPMENT REPORT, DECEMBER 2011, ACCESSED JULY 2017 FROM URL HTTPS://STON.JSC.NASA.GOV/COLLECTIONS/TRS/_TECHREP/TM-2011-216163.PDF
[6] HATHAWAY, JACOB D., AND JAMEY D. JACOB. "DEVELOPMENT OF A MICROGRAVITY GENERATING FLIGHT MODE FOR UAS." AIAA MODELING AND SIMULATION TECHNOLOGIES CONFERENCE. 2016.

AFTER AN OVERVIEW OF "TYPE 3" SYSTEMS, ONE COULD SAY THAT THE TYPE OF CONTROL LAW EMPLOYED DID NOT EAT IT'S CHEERIOS.

WHAT DID WE LEARN?

WHAT DO THESE PREVIOUS ATTEPMTS HAVE IN COMMON?

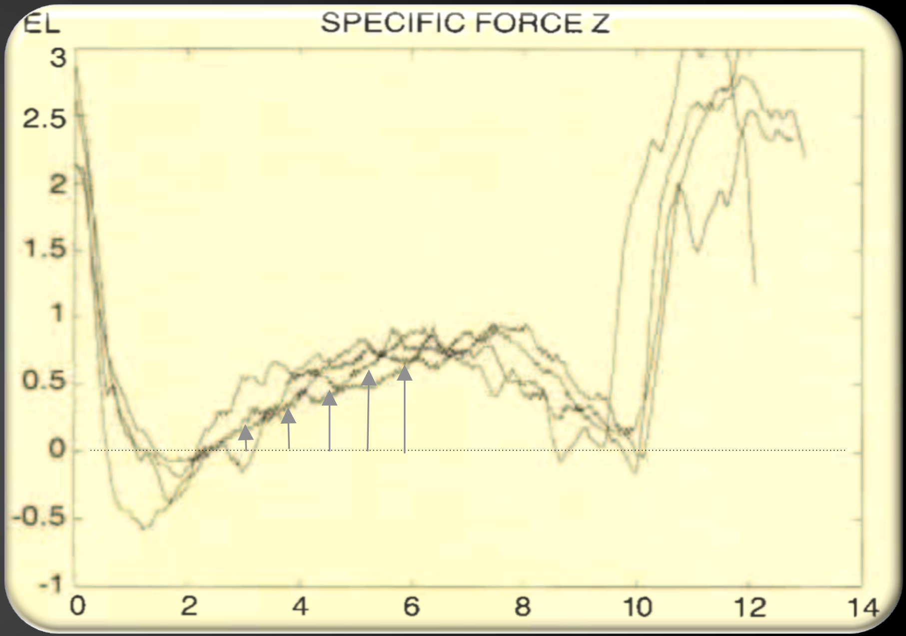

DEVIATION OCCURS DUE TO A DISTURBANCE WITH PARABOLIC GROWTH

- 22 YEARS OF EFFORTS EMPLOYING THE SAME CONTROL ARCHITECTURE
- FLAW REVEALED AT THE LEVEL OF MODEL BASED DESIGN

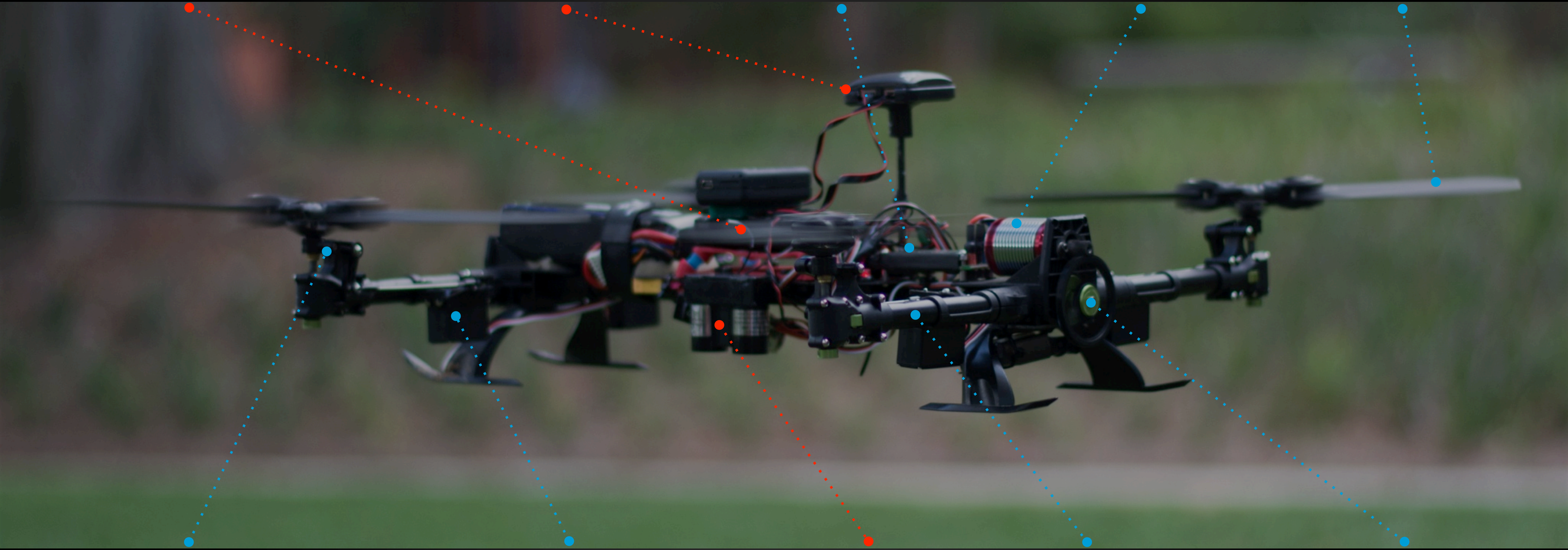
CONTROL FIRMWARE
GPS
SPEED GOVERNOR
SINGLE MOTOR
SYMMETRIC BLADES
VARIABLE PITCH
SERVO CONTROL
LIDAR
BELT DRIVEN
DRIVE SHAFT

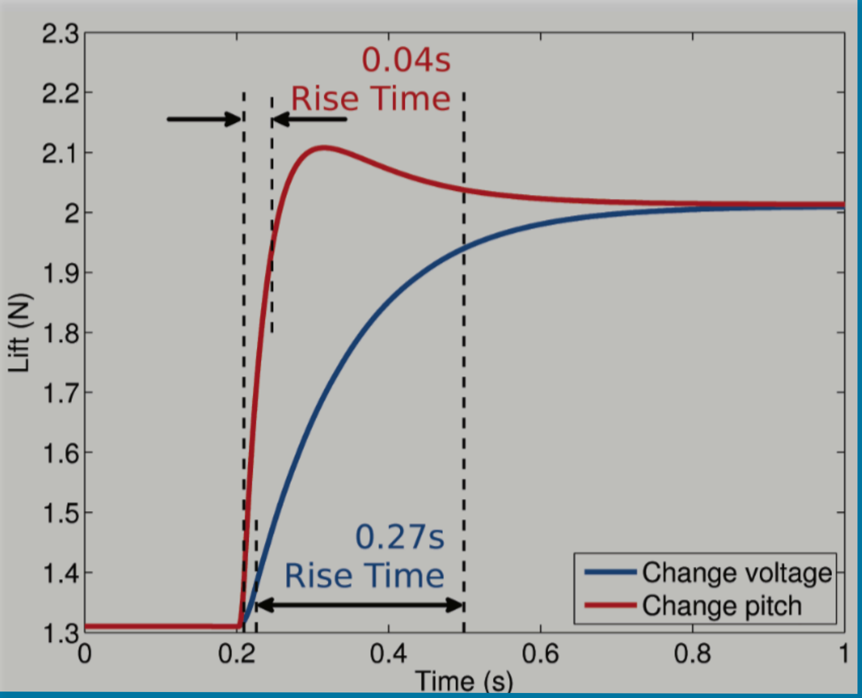

WHY VARIABLE-PITCH PROPULSION?

WHAT MAKES VARIABLE PITCH SEXY FOR PARABOLIC MANEUVERS?

Most of us are familiar with fixed-pitch multi-rotors, but what makes the unconventional variable-pitch system a better fit for parabolic maneuvers?

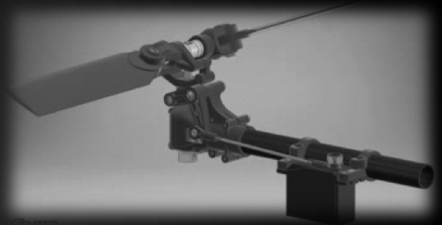

Increased control bandwidth and disturbance rejection.

-Operating at constant RPM implies faster response over conventional fixed pitch configuration due to rotational inertia of motor-propeller combination

-Fast response improves precision and tracking

Positive and negative thrust enables dynamic inversion of the drag disturbance for both sides of the parabolic maneuver

-We need to fight disturbances on the way up and on the way down!!

Control authority is independent of thrust.

-We tried fixed pitch… the results were amusing!

WHY VARIABLE-PITCH PROPULSION?

WHAT MAKES VARIABLE PITCH SEXY FOR PARABOLIC MANEUVERS?

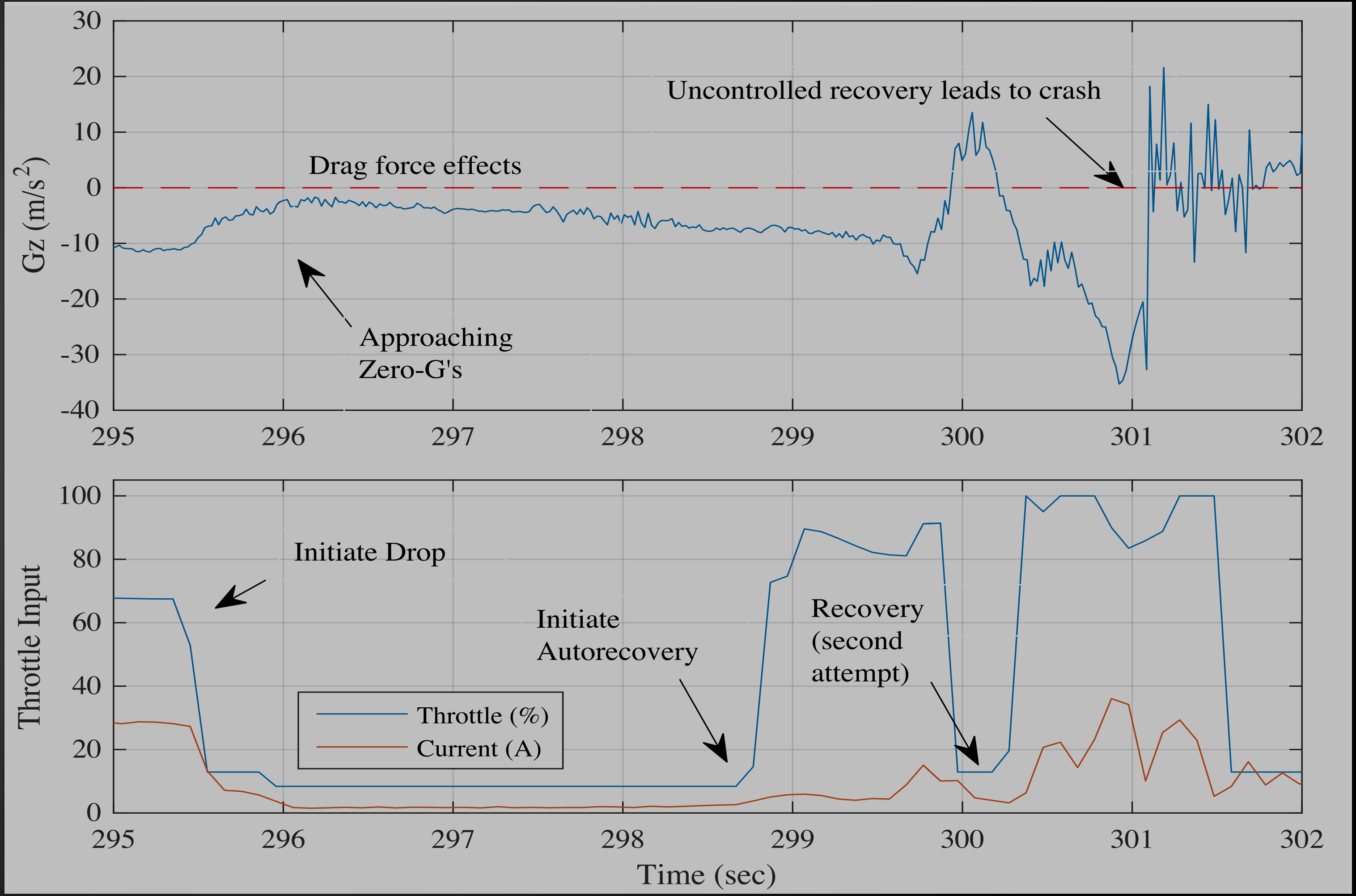

MODEL BASED DESIGN FRAMEWORK

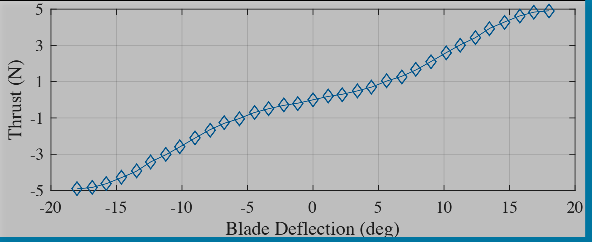

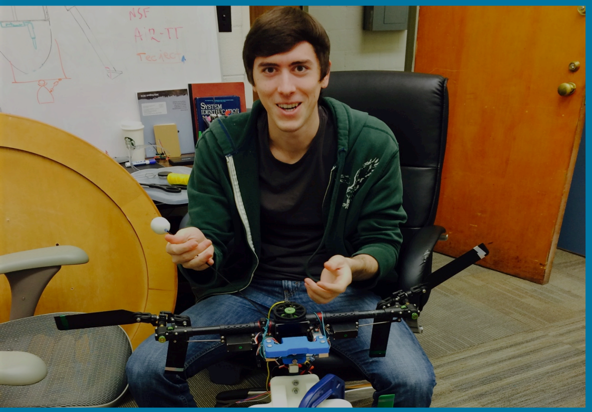

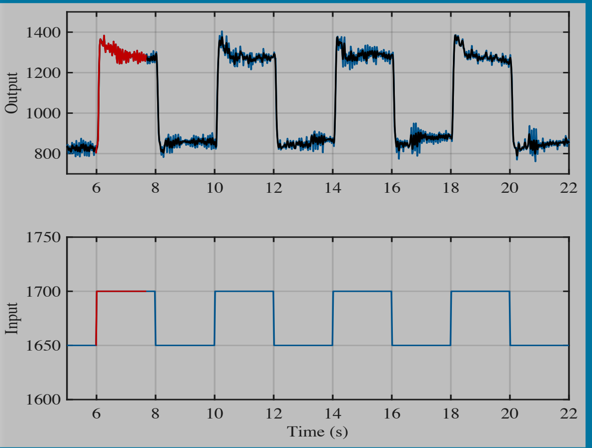

MODEL-BASED DESIGN FRAMEWORK

FULLY IDENTIFIED-*ISH* SYSTEM

Parameter	Estimate
I_{xx}	$0.0068\ (kg \cdot m^2)$
I_{yy}	$0.0171\ (kg \cdot m^2)$
I_{zz}	$0.0207\ (kg \cdot m^2)$
m	$1.265\ (kg)$

CONTROL LAW & MODE

SERVO DEADBAND

AERO MODELS

FORCES , MOMENTS & IDENTIFIED PARAMETERS

VISUALIZATION

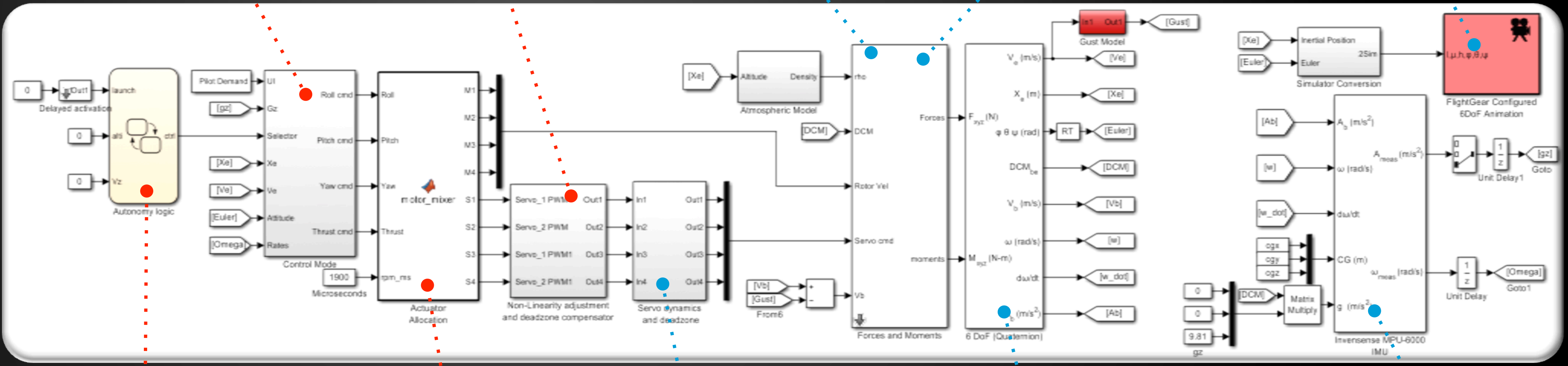

AUTOMATA

ACTUATOR ALLOCATION

$$G_p(s) = \frac{1}{0.0008s^2 + 0.045s + 1}$$

SERVO DYNAMICS

RIGID BODY EOM

SENSOR DYNAMICS

MODEL-BASED DESIGN FRAMEWORK

CONTROL LAWS

SERVO DEADBAND

AERO MODELS

FORCES , MOMENTS & IDENTIFIED PARAMETERS

VISUALIZATION

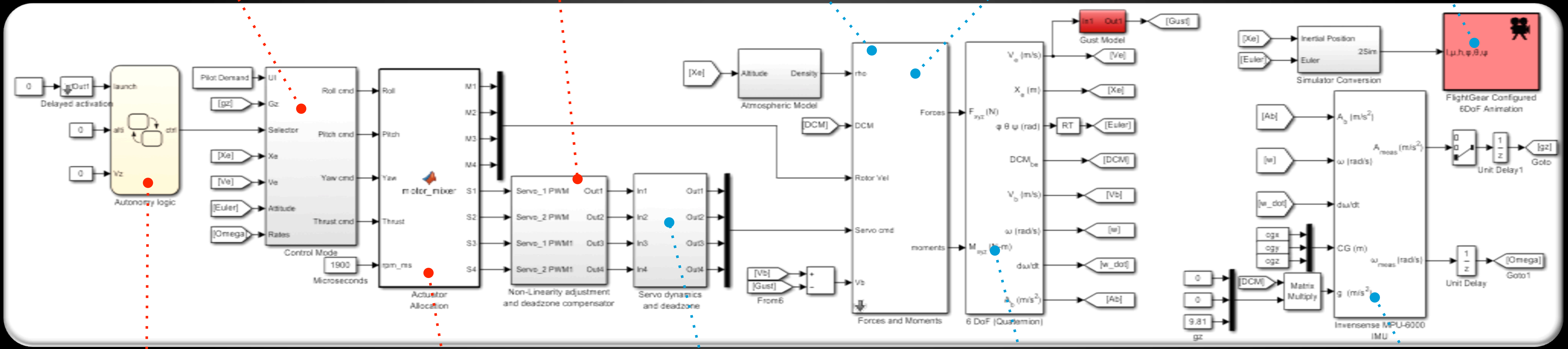

AUTOMATA

ACTUATOR ALLOCATION

SERVO DYNAMICS

RIGID BODY EOM

SENSOR DYNAMICS

AUTONOMY STATE TRANSITION LOGIC FOR AUTONOMOUS MANEUVER

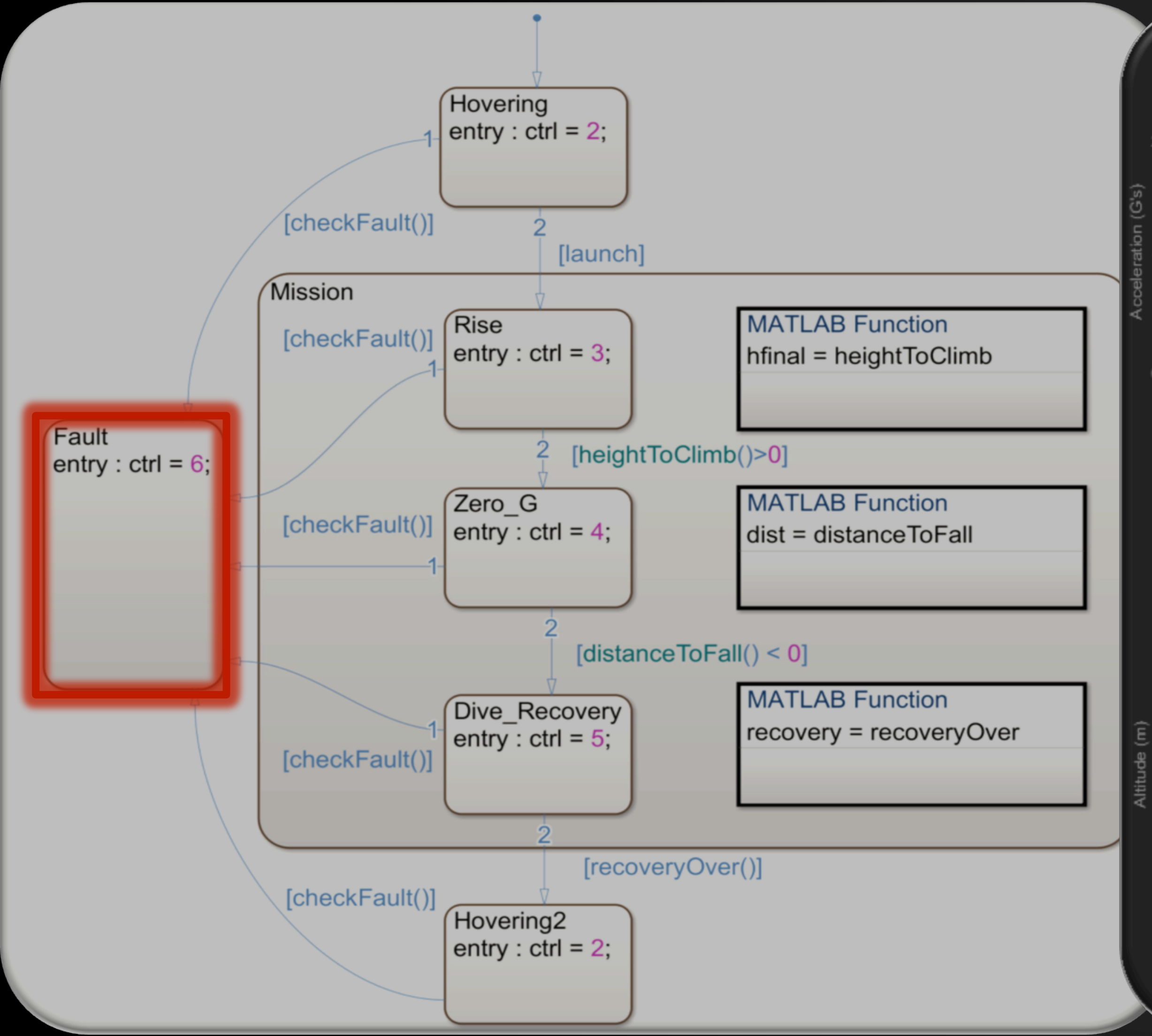

AUTOMATA

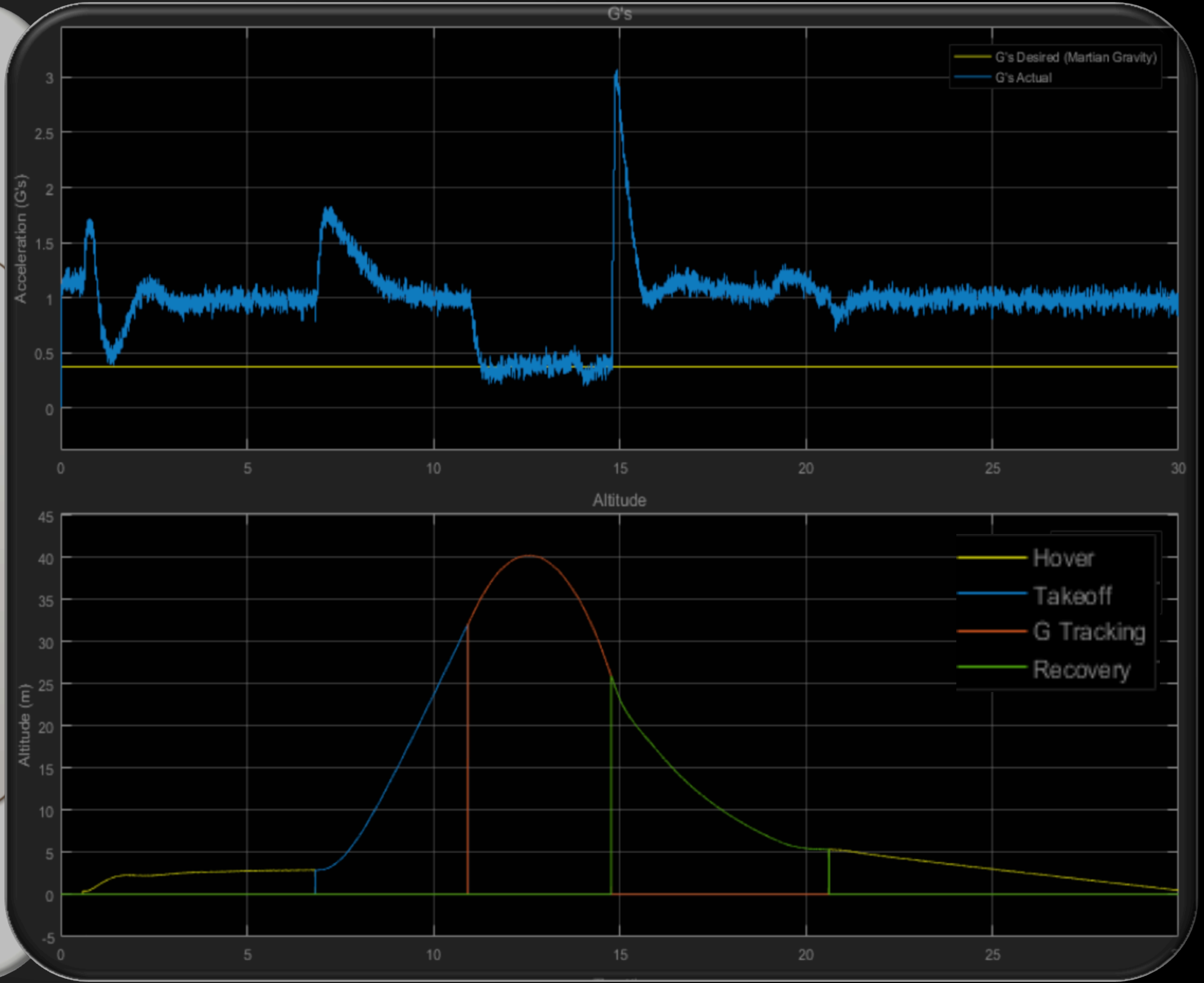

MANEUVER

SAFETY REAL TIME FAULT DETECTION LOGIC

BELT SLIP OR SERVO FAULT

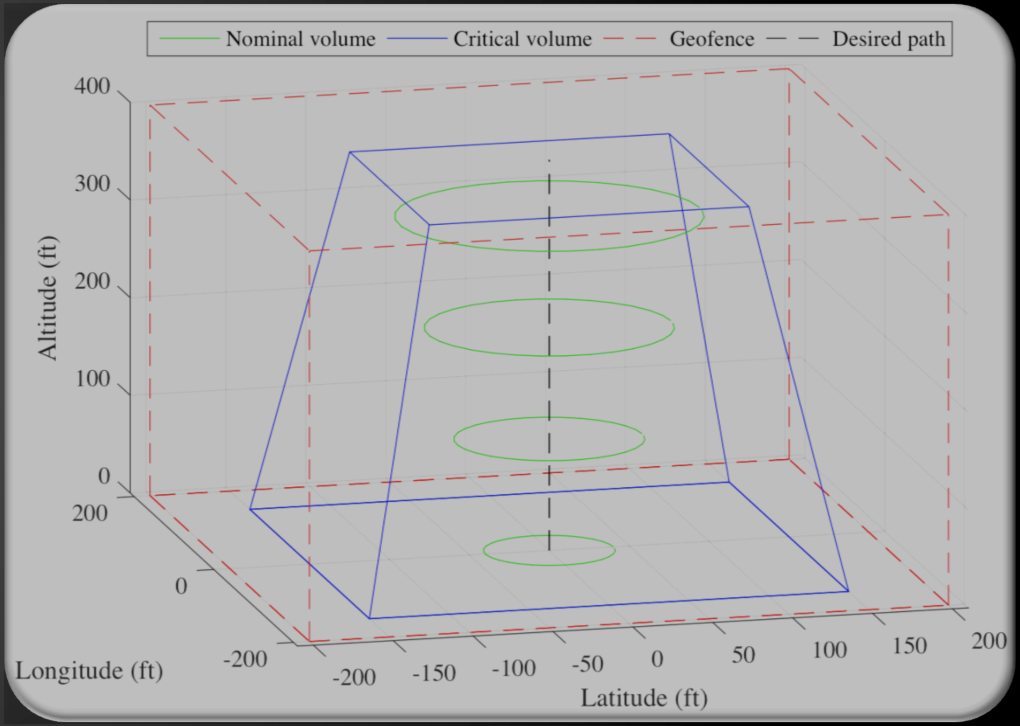

GEOFENCE

https://youtu.be/J5tkTEnAiyA

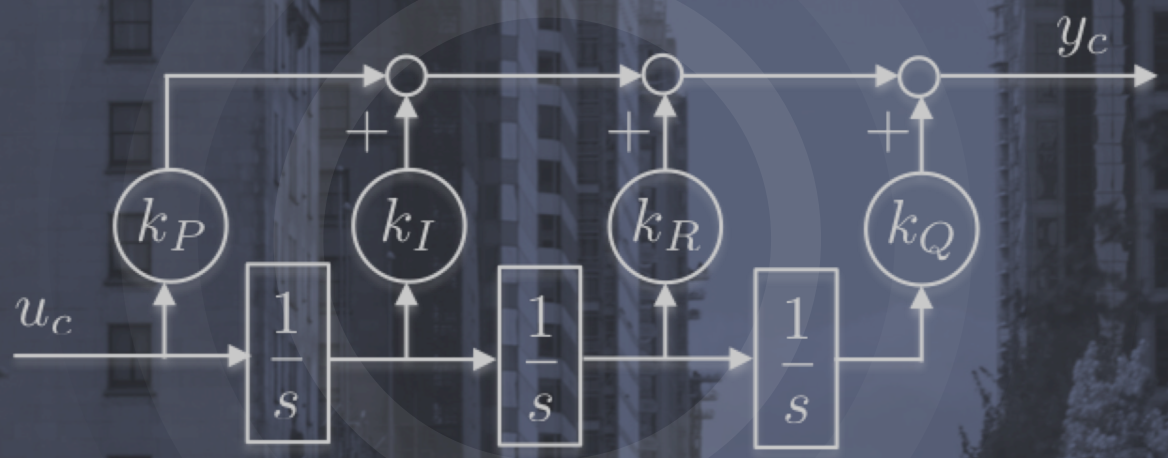

REDUCED-G MANEUVERING AND THE *TRIPLE INTEGRAL CONTROL LAW*

ANALYSIS OF FREE FALL MANEUVERS

PIRQ CONTROL LAW ANALYSIS OF AN IDEAL FREE-FALL MANEUVER

$$D \propto v^2$$

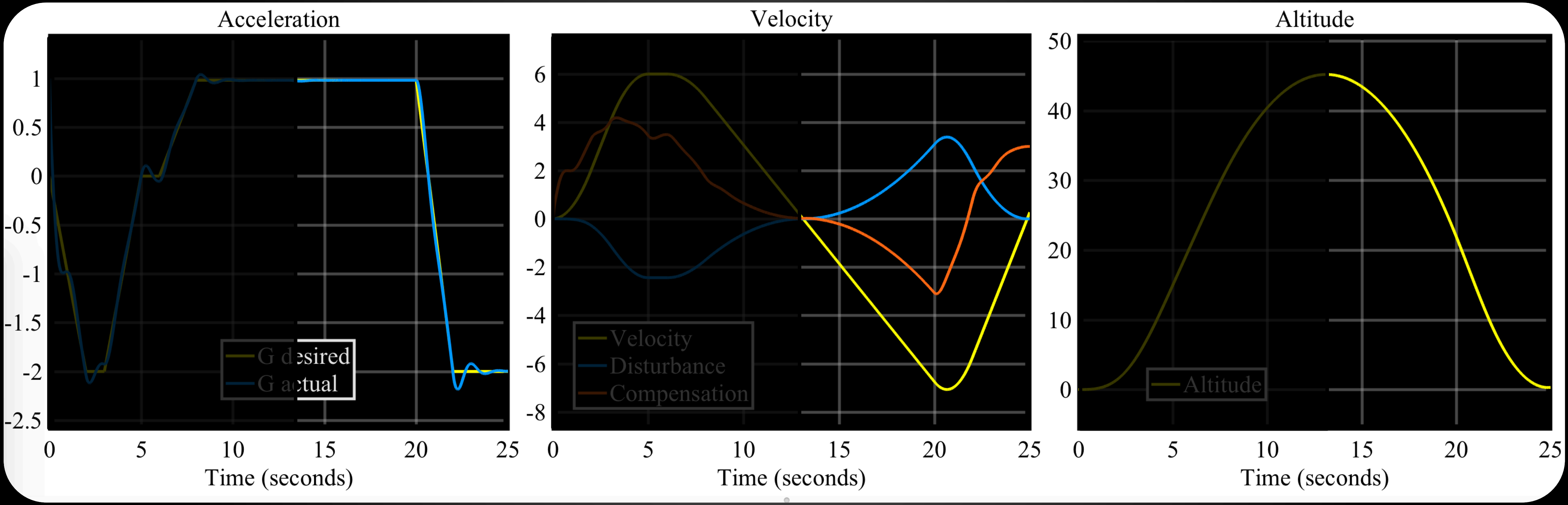

→Goal: Provide automatic **compensation of the naturally occurring drag force through dynamic inversion**

When $a_d = 1g$, the goal is indeed free fall.

PIRQ CONTROL LAW ANALYSIS OF AN IDEAL FREE-FALL MANEUVER

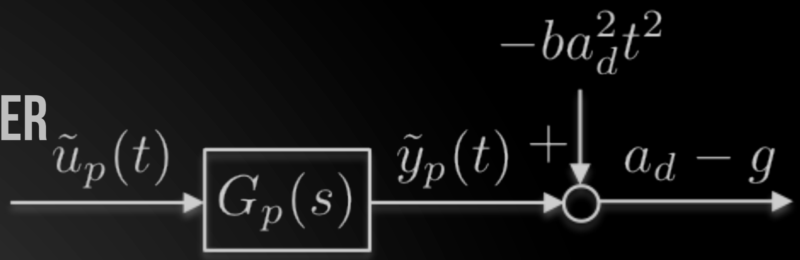

Consider an ideal trajectory trajectory with

$$\tilde{v}(t) = a_d\, t$$

The output of the propulsive system needs to be

$$\tilde{y}_p(t) = b a_d^2\, t^2 + a_d - g$$

The state $\tilde{x}_p(t)$ and input $\tilde{u}_p(t)$ trajectories corresponding to this quadratic output $\tilde{y}_p(t)$ are also quadratic, with the form:

$$\tilde{x}_p(t) = x_0 + x_1\, t + x_2\, t^2/2$$
$$\tilde{u}_p(t) = u_0 + u_1\, t + u_2\, t^2/2$$

where each coefficient is determined by enforcing:

$$\dot{\tilde{x}}_p(t) = A_p\, \tilde{x}_p(t) + b_p\, \tilde{u}_p(t)$$
$$c_p\, \tilde{x}_p(t) = b a_d^2\, t^2 + a_d - g$$

The state and input of Gp(s) provide dynamic inversion of the quadratic disturbance.

Lemma 1: Let $G(s) = c^T(sI - A)^{-1}b$ be stable with $G(0) = 1$. Then every polynomial output $y(t) = y_0 + y_1 t + \cdots + y_k t^k/k!$ can be produced with a corresponding polynomial input $u(t) = u_0 + u_1 t + \cdots + u_k t^k/k!$ and state $x(t) = x_0 + x_1 t + \cdots + x_k t^k/k!$.

$$\begin{aligned}
u_2 &= \;\; 2ba_d^2 \\
x_2 &= -2ba_d^2\, A_p^{-1} b_p \\
u_1 &= \;\; 2ba_d^2\, c_p^T A_p^{-2} b_p \\
x_1 &= -2ba_d^2\, (A_p^{-2} b_p + c_p^T A_p^{-2} b_p\, A_p^{-1} b_p) \\
u_0 &= \;\; 2ba_d^2\, (c_p^T A_p^{-3} b_b + (c_p^T A_p^{-2} b_p)^2) \; + \; a_d - g \\
x_0 &= -2ba_d^2\, [A_p^{-3} b_p + c_p^T A_p^{-2} b_p\, A_p^{-2} b_p \\
&\qquad + (c_p^T A_p^{-3} b_b + (c_p^T A_p^{-2} b_p)^2)\, A_p^{-1} b_p] \\
&\qquad - A_p^{-1} b_p\, (a_d - g)
\end{aligned}$$

PIRQ CONTROL LAW ANALYSIS OF AN IDEAL FREE-FALL MANEUVER

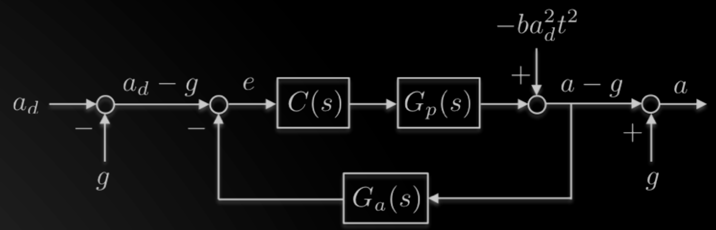

The required quadratic input $\tilde{u}_p(t)$ for the drag compensated maneuver should be provided by the controller output $\tilde{y}_c(t)$ under *zero* input $\tilde{u}_c(t) \equiv 0$

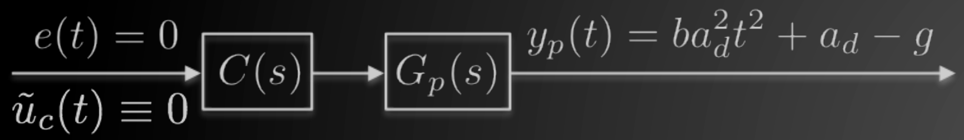

This can be accomplished using a chain of three integrators, providing constant (or step), linear (or ramp), and quadratic components in its output under zero input conditions.

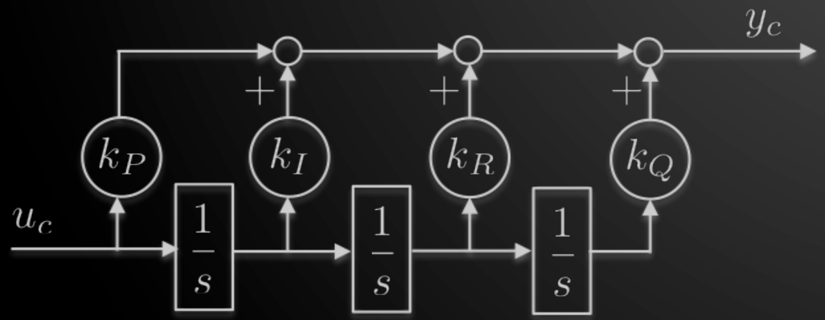

The transfer function of this *PIRQ* (Proportional-Integral-Ramp-Quadratic) controller is

$$C(s) = \frac{k_P s^3 + k_I s^2 + k_R s + k_Q}{s^3}$$

with state space realization

$$\left[\begin{array}{c|c} A_c & b_c \\ \hline c_c^T & d_c \end{array}\right] = \left[\begin{array}{ccc|c} 0 & 1 & 0 & 0 \\ 0 & 0 & 1 & 0 \\ 0 & 0 & 0 & 1 \\ \hline k_Q & k_R & k_I & k_P \end{array}\right]$$

where the PIRQ coefficients are all positive (and subject to some stability conditions)

PIRQ CONTROL LAW ANALYSIS OF AN IDEAL FREE-FALL MANEUVER

With zero input, the controller state has the form

$$\tilde{x}_c(t) = \begin{bmatrix} q_0 + r_0 t + s_0 t^2/2 \\ r_0 + s_0 t \\ s_0 \end{bmatrix}$$

Note that by equating the controller output with the maneuver actuator input, we find the required controller's I.C.

$$\tilde{x}_c(0) = \begin{bmatrix} q_0 \\ r_0 \\ s_0 \end{bmatrix} = \begin{bmatrix} \frac{1}{k_Q}\left(u_0 - \frac{k_R}{k_Q}u_1 + \frac{k_R^2 - k_I k_Q}{k_Q^2}u_2\right) \\ \frac{1}{k_Q}\left(u_1 - \frac{k_R}{k_Q}u_2\right) \\ \frac{1}{k_Q}u_2 \end{bmatrix}$$

This shows that the controller and actuator are capable of providing the necessary signals to compensate the drag in an ideal maneuver.

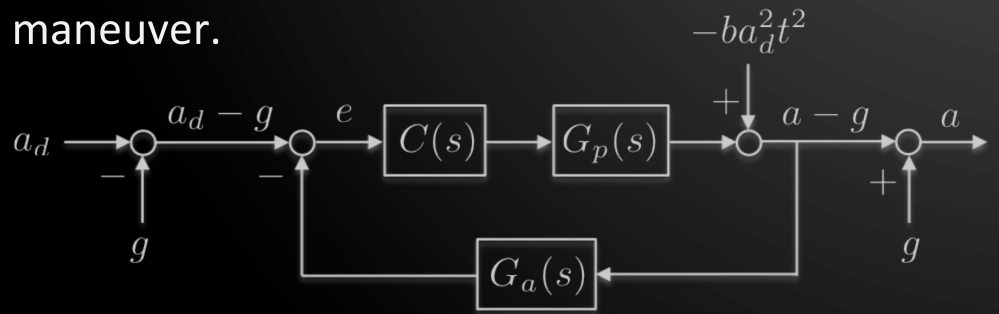

This control system can be used to determine, in a feedback manner, the internal trajectory leading to asymptotic rejection of the *disturbance* $-ba_d^2 t^2$ without knowledge of b (or even a_d)

Here $1/s^3$ provides an *internal model* for the (idealized maneuver drag) disturbance t^2.

Asymptotic disturbance rejection is obtained for the linear feedback system provided that $C(s)$ stabilizes the feedback loop, possible when $G_p(s)$ and $G_a(s)$ are *exponentially* stable and minimum phase. This is accomplished by choosing the location of the zeros

$$s^3 + \frac{k_I}{k_P}s^2 + \frac{k_R}{k_P}s + \frac{k_Q}{k_P}$$

and the gain K_p to bring the three compensator poles (at 0) into the open left half plane.

LOOP-SHAPING IMPLEMENTATION

Although the tracking performance analysis should involve only the forward gain $C(s)G_p(s)$, the forward gain $C(s)G_p(s)G_a(s)$ was employed bearing in mind that the dynamic range of the accelerometer largely exceeds that of the eventual closed-loop system bandwidth.

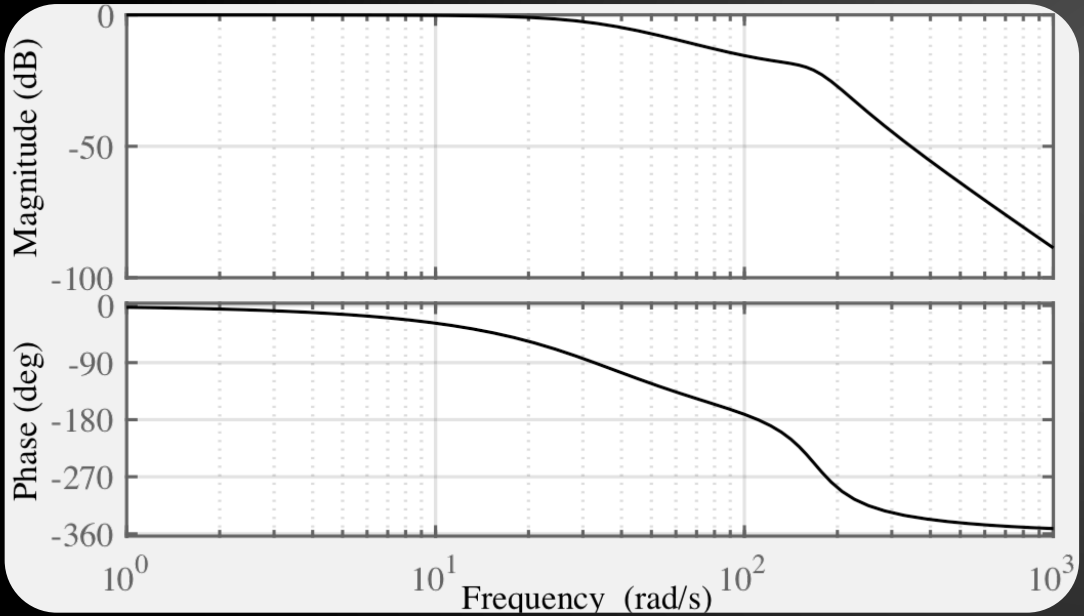

Frequency response of the uncontrolled loop-gain

For the compensated linear system $K_pG_p(s)G_a(s)/s^3$

- While the gain slope of -60 dB/dec at low frequencies ensures ability of rejecting quadratic disturbance,

-There exists no gain that yields positive phase margin.

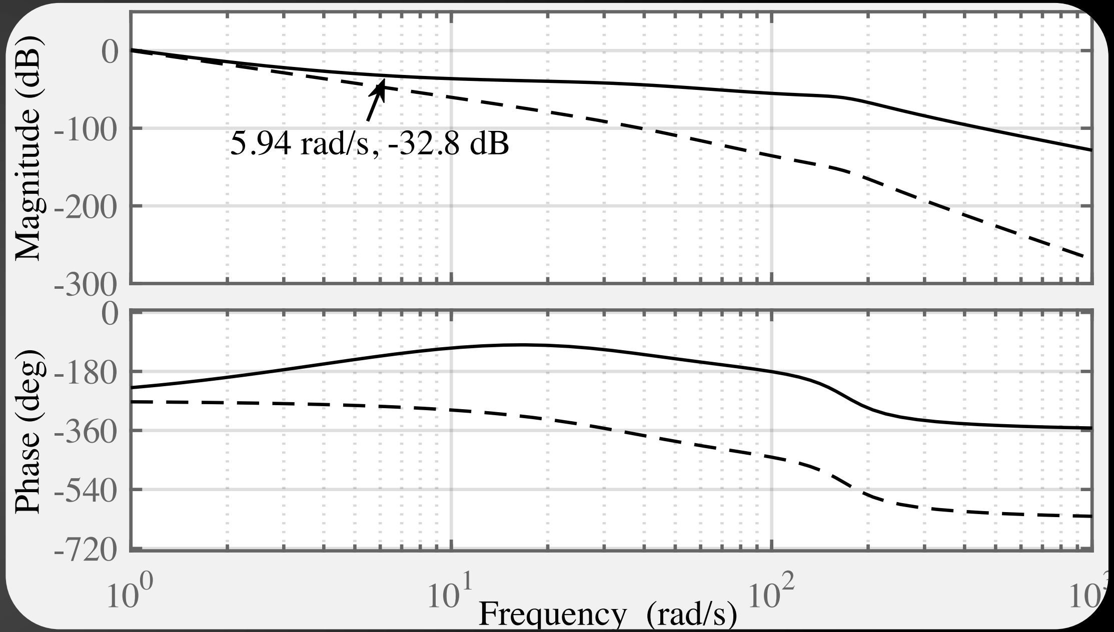

Frequency response of the compensated linear system

This is addressed by the introduction of three zeros. The choice of zeros is dependent upon the desired bandwidth and should consider high-frequency sensor noise attenuation.

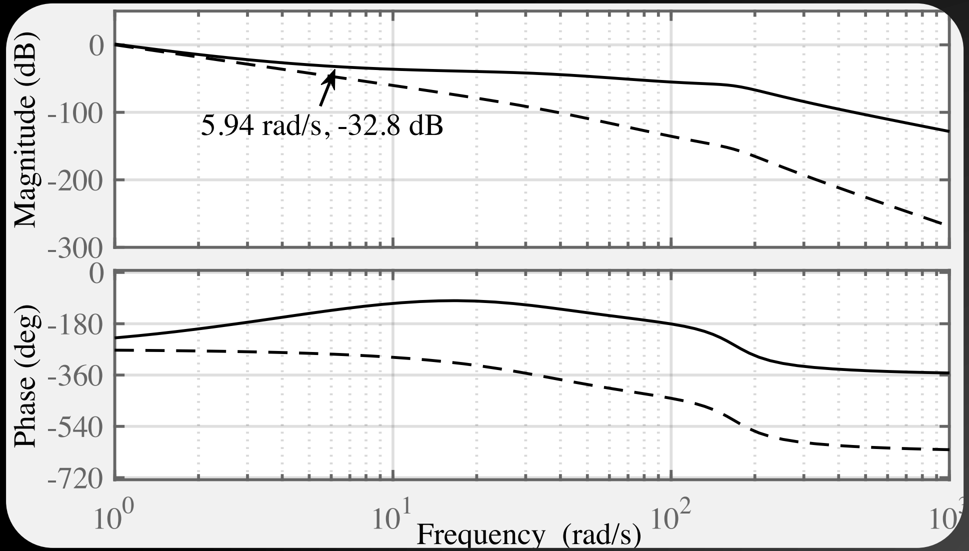

Frequency response of the compensated linear system

The compensated loop-gain now displays desirable properties, including a positive phase margin from 3 to 90 rad/sec. Furthermore, the range of Kp for which closed-loop stability is possible can be seen in the corresponding root-locus

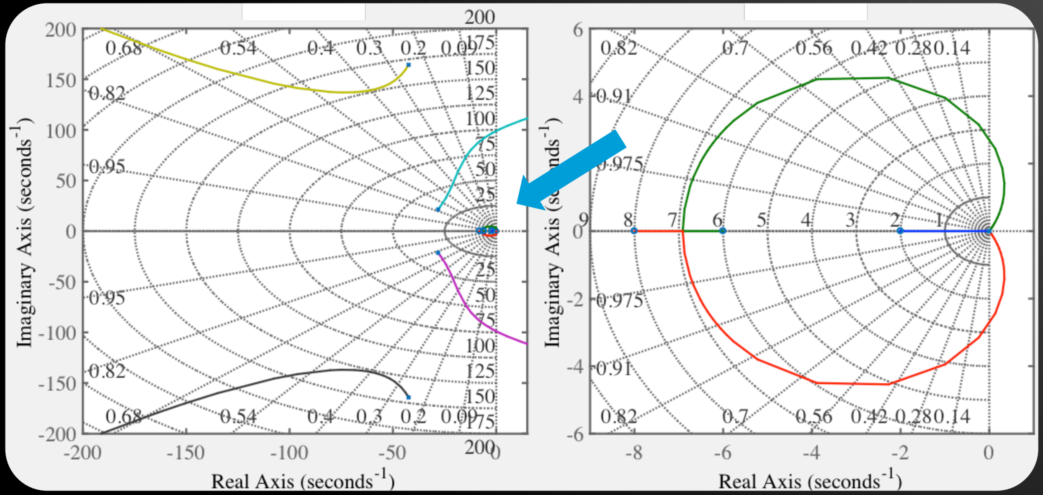

10.5 < Kp < 562 stabilizes the linear system.

Alternating between flight tests and design, the crossover frequency was placed at 5.94 rad/sec

-Results based on our identified linear system

-Resulting in a phase margin of 46.3 deg.

-It is suspected that the actual system's phase margin is higher than this, but with a discrepancy due to modeling uncertainty.

The compensated loop gain was adjusted by factor of 32.8 dB.

$$C(s) = \frac{k_P s^3 + k_I s^2 + k_R s + k_Q}{s^3}$$

$k_P = 0.40$ | $k_I = 6.40$ | $k_R = 30.40$ | $k_Q = 38.40$

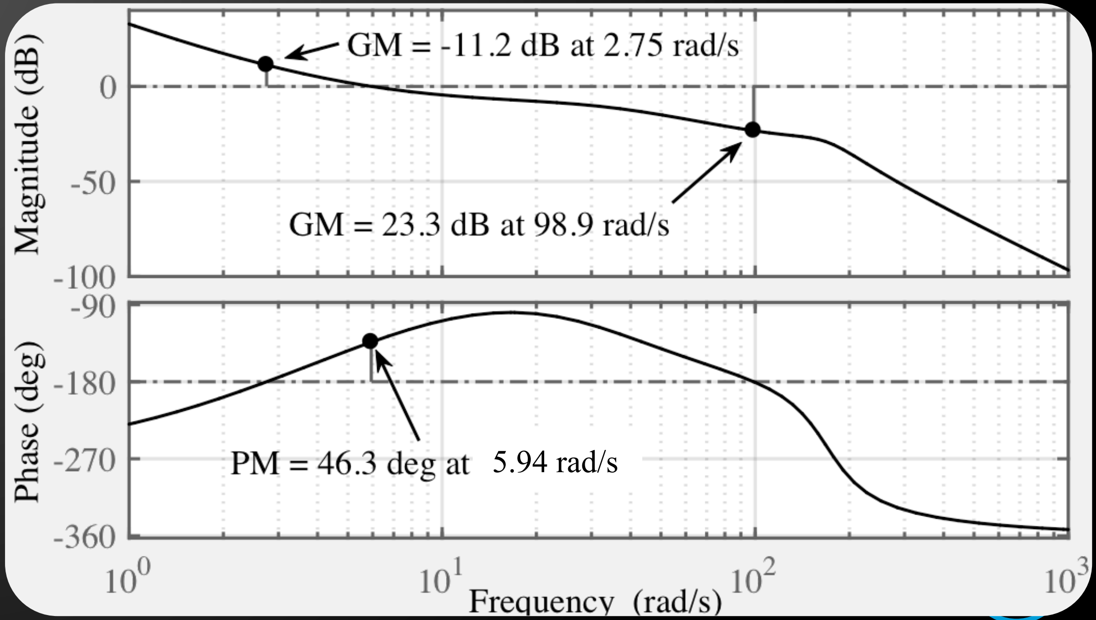


I WOULD LIKE TO DIE ON MARS...
...JUST NOT ON IMPACT.
-ELON MUSK
THE MARTIAN MANEUVER

ON JULY 14TH, 2017, OUR TEAM PERFORMED THE FIRST AUTONOMOUS REDUCED-G PARABOLA

https://youtu.be/-sSCuPzgb3g

Effect from not resetting integrators – We have hybrid system work to do during toss-fall transition

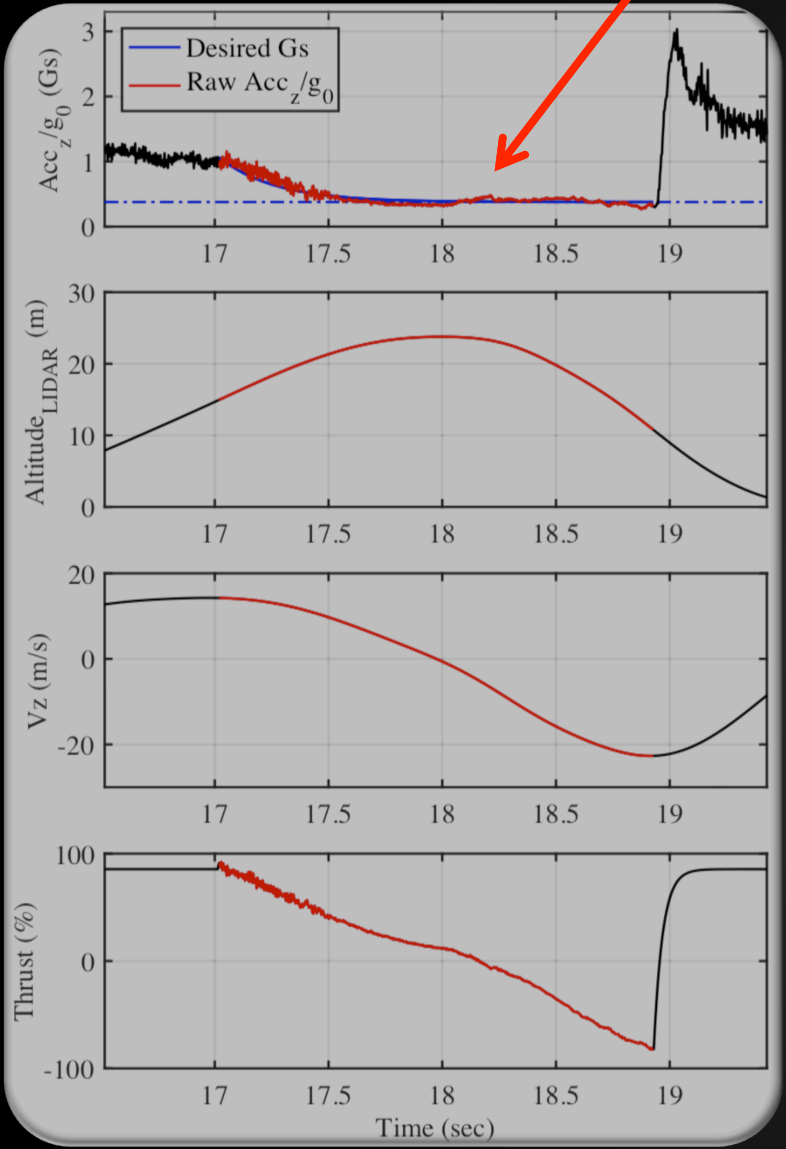

MARTIAN MANEUVER

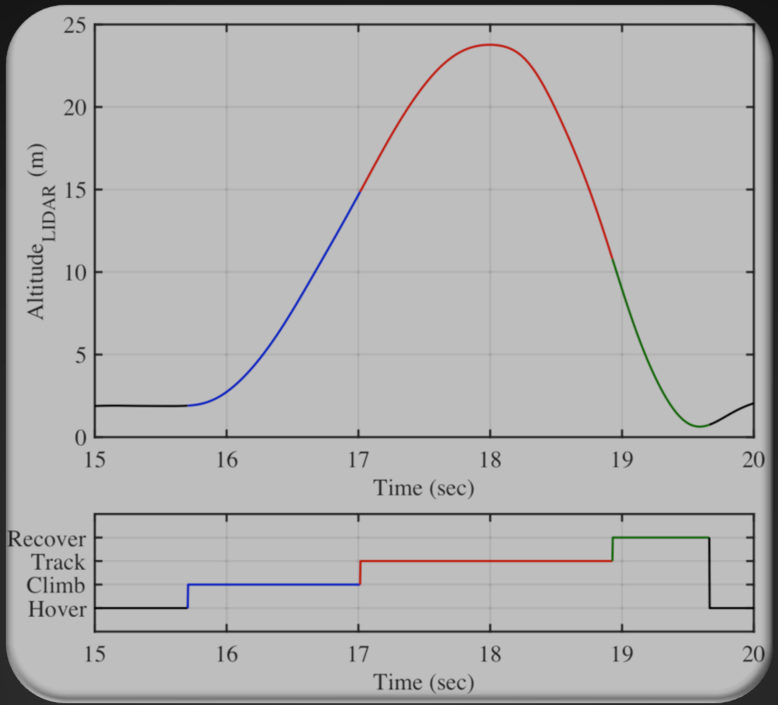

MARTIAN TEMPORAL PARABOLA

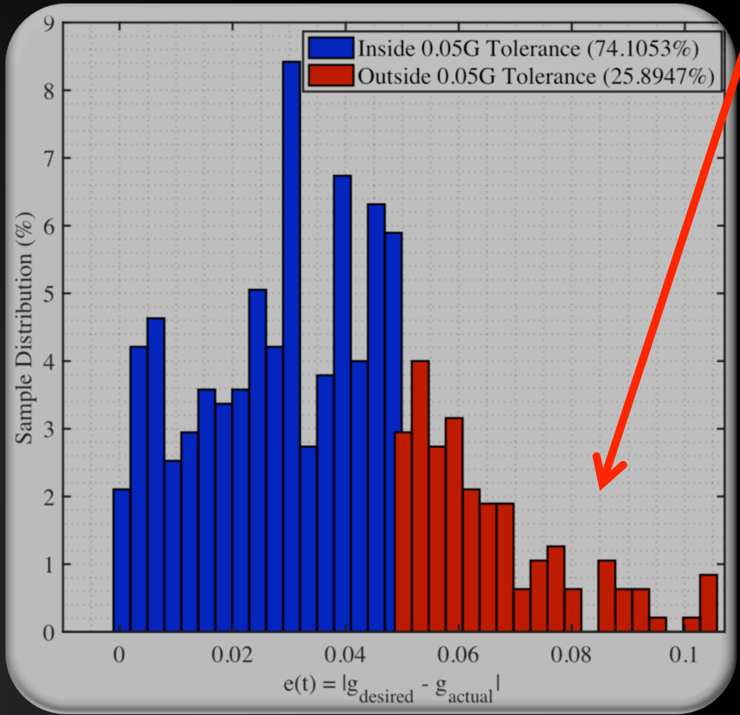

ERROR ANALYSIS

THE ACCURACY OF EXPERIMENTAL PARABOLA CONTAINED TOLERANCES WITHIN ±0.1*G* FOR A PERIOD OF APPROXIMATELY 1.5 SECONDS, WITH A MEAN OF 0.3804 AND STANDARD DEVIATION OF 0.0426.

TO DO: HYBRID SYSTEM DURING TOSS-FALL TRANSITION

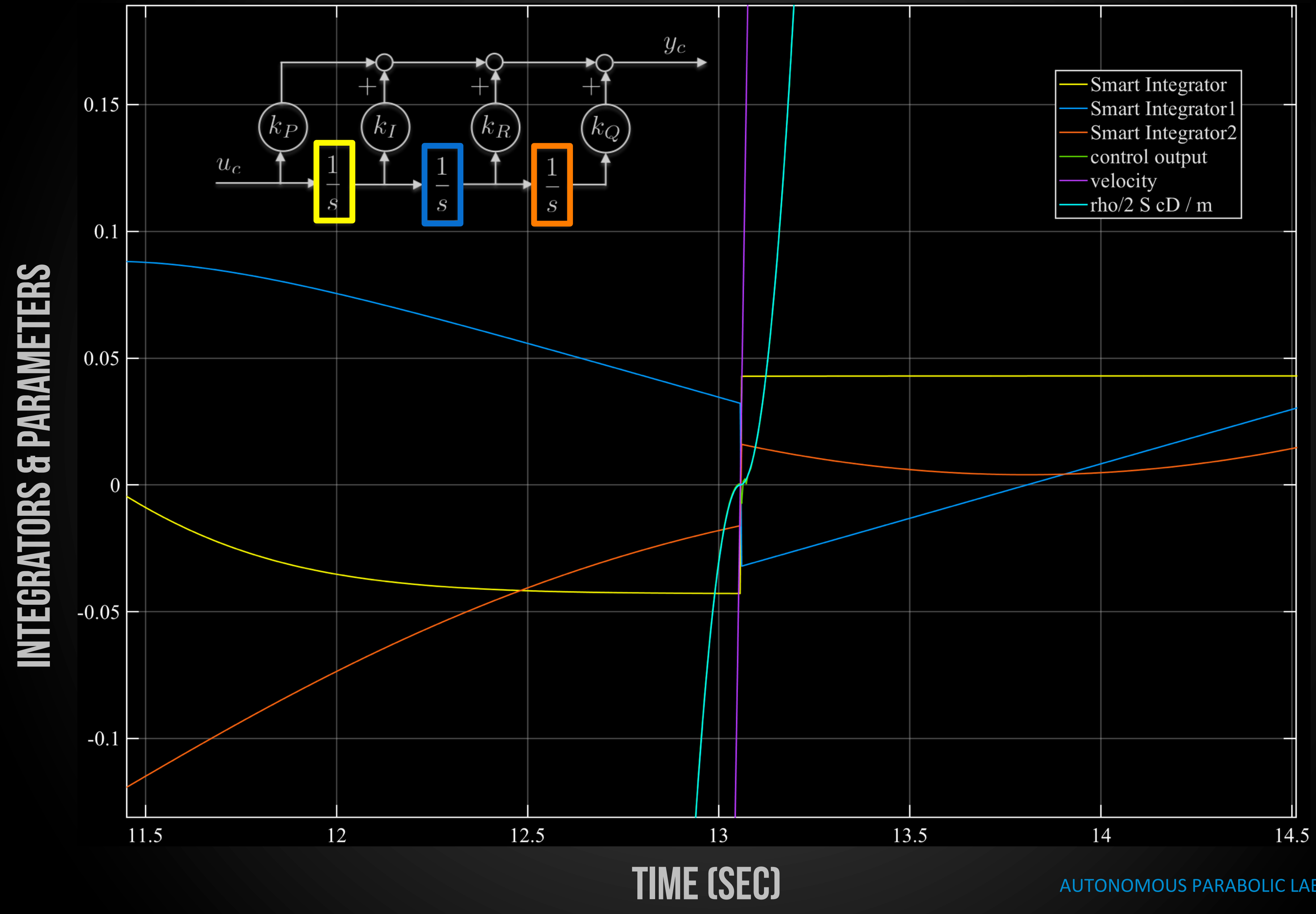

PIRQ CONTROL LAW MANEUVER

In reality, the drag disturbance is not ideal,

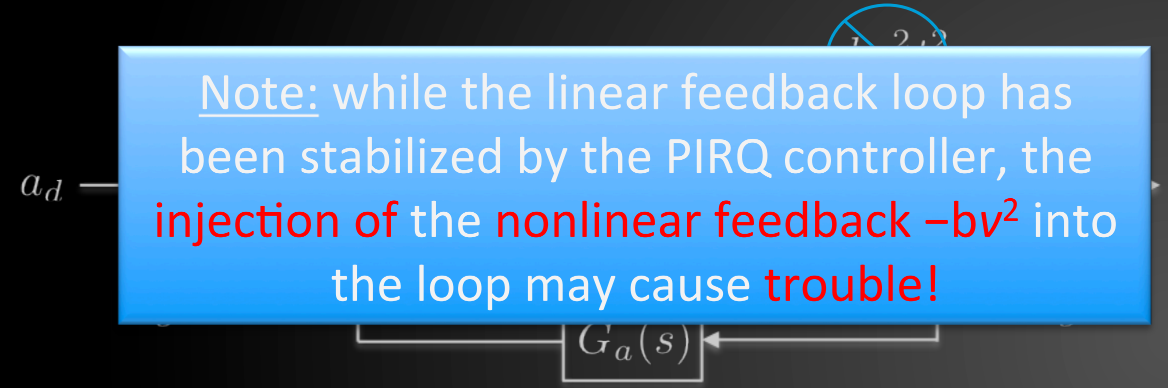

<u>Note:</u> while the linear feedback loop has been stabilized by the PIRQ controller, the injection of the nonlinear feedback $-bv^2$ into the loop may cause trouble!

but dependent on the velocity state v

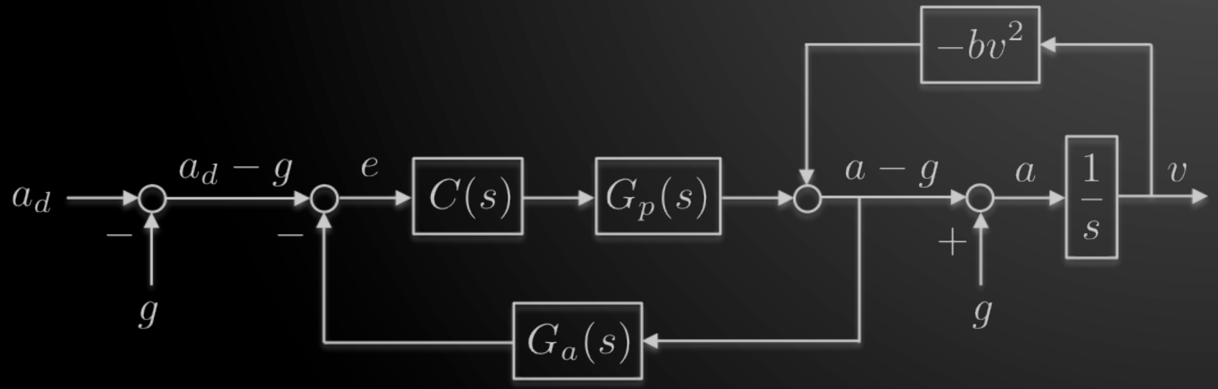

$$\dot{v} = c_p^T x_p - bv^2 + g \quad (1)$$

$$\begin{bmatrix} \dot{x}_p \\ \dot{x}_c \\ \dot{x}_a \end{bmatrix} = \begin{bmatrix} A_p & b_p c_c^T & -b_p d_c c_a^T \\ 0 & A_c & -b_c c_a^T \\ b_a c_p^T & 0 & A_a \end{bmatrix} \begin{bmatrix} x_p \\ x_c \\ x_a \end{bmatrix} + \begin{bmatrix} b_p d_c \\ b_c \\ 0 \end{bmatrix} (a_d - g) + \begin{bmatrix} 0 \\ 0 \\ -b_a b v^2 \end{bmatrix} \quad (2)$$

Here, we note that

$$(v, x_p, x_c, x_a)(t) = (a_d t, \tilde{x}_p(t), \tilde{x}_c(t), \tilde{x}_a)$$

is a trajectory of the system.

-Trajectory: is a curve traced out in our state space by our desired *maneuver.*

-Invariant curve of the dynamics in the state space.

TRANSVERSE COORDINATES

What we would like is to make the desired maneuver ***exponentially attractive***.

- $\tilde{v}(t) = a_d t$ is monotonically increasing (for $a_d > 0$),
- we may use its inverse $t(v) = v/a_d$ to provide maneuver parameterization by v.

By defining:
$$\begin{cases} \bar{x}_p(v) = \tilde{x}_p(\bar{t}(v)) \\ \bar{x}_c(v) = \tilde{x}_c(\bar{t}(v)) \\ \bar{x}_a = \tilde{x}_a \end{cases}$$

We obtained the desired maneuver

$$(v, \bar{x}_p(v), \bar{x}_c(v), \bar{x}_a) = (v, \bar{x}(v)), v \geq 0.$$

Maneuver adapted transverse coordinates as stable invariant set

$$\begin{cases} x_p = \bar{x}_p(v) + z_p \\ x_c = \bar{x}_c(v) + z_c \\ x_a = \bar{x}_a + z_a \end{cases}$$

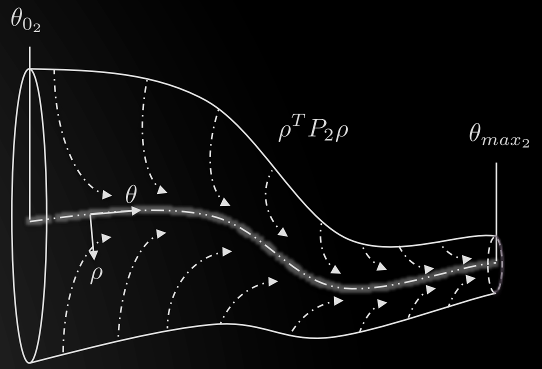

$$\dot{v} = a_d + c_p^T z_p$$

$$\begin{bmatrix} \dot{z}_p \\ \dot{z}_c \\ \dot{z}_a \end{bmatrix} = \begin{bmatrix} A_p - \bar{x}_p'(v) c_p^T & b_p c_c^T & -b_p d_c c_a^T \\ -\bar{x}_c'(v) c_p^T & A_c & -b_c c_a^T \\ b_a c_p^T & 0 & A_a \end{bmatrix} \begin{bmatrix} z_p \\ z_c \\ z_a \end{bmatrix}$$

And tangential coordinates evolving at the same rate as time when on the maneuver. $\theta = v/a_d$

$$\begin{cases} \dot{\theta} = 1 + (1/a_d)\, \bar{c}^T \rho \\ \dot{\rho} = (\bar{A} - 2b a_d\, \bar{x}_1 \bar{c}^T - 2b a_d\, \bar{x}_2\, \theta\, \bar{c}^T)\, \rho \end{cases}$$

MANEUVER AS STABLE INVARIANT SET

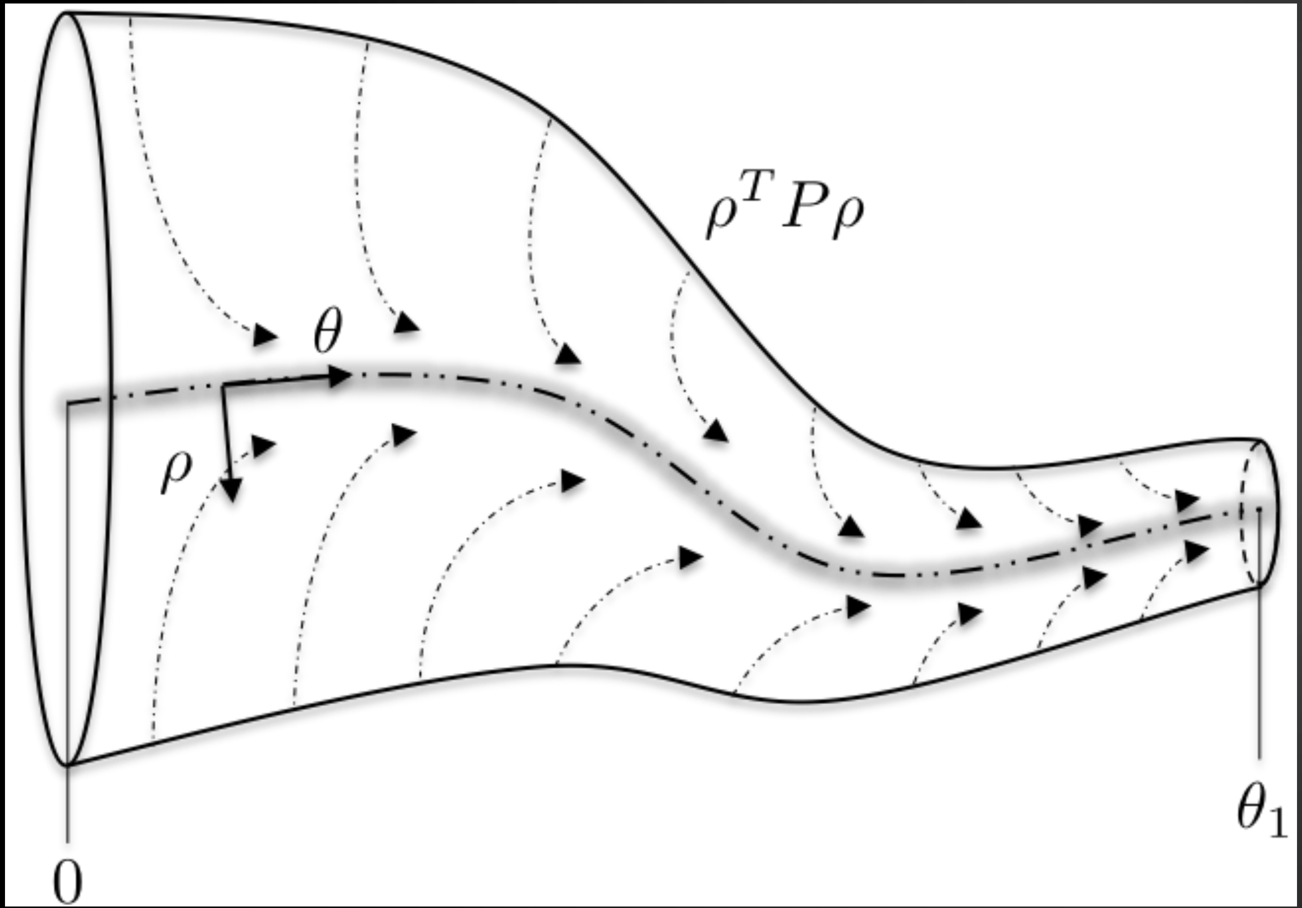

$$\dot{\theta} = 1 + (1/a_d)\,\bar{c}^T \rho$$
$$\dot{\rho} = (\bar{A} - 2ba_d\,\bar{x}_1\bar{c}^T - 2ba_d\,\bar{x}_2\,\theta\,\bar{c}^T)\,\rho =: A(\theta)\,\rho$$

$$V(\rho) = \rho^T P \rho$$

$$A(\theta)^T P + P A(\theta) + Q \leq 0$$

$$\dot{V}(\theta,\rho) = \rho^T (A(\theta)^T P + P A(\theta))\,\rho \leq -\rho^T Q \rho < 0.$$

CURRENT WORK

AUTOMATA – STABILITY GUARANTEES ACROSS STATE TRANSITION LOGIC
OR
ACROSS HYBRID SYSTEM TRANSITIONS

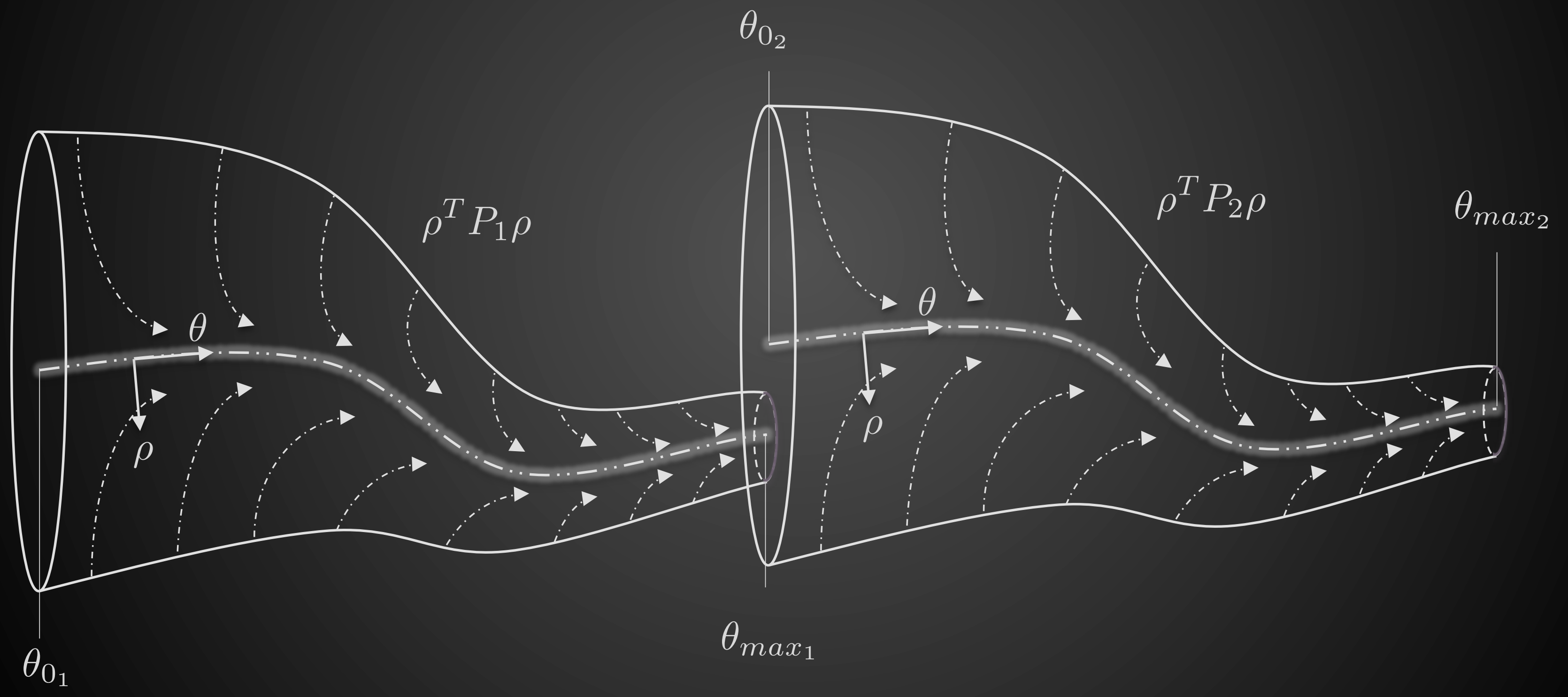

THANK YOU

PLEASE STAY IN TOUCH!

jafman3@gatech.edu

skype.com/jafman33